

Characteristics of Retinal Nerve Fiber Layer Defect in Nonglaucomatous Eyes With Type II Diabetes

Soo Ji Jeon,¹ Jin-Woo Kwon,¹ Tae Yoon La,¹ Chan Kee Park,² and Jin A Choi¹

¹Department of Ophthalmology, St. Vincent's Hospital, College of Medicine, Catholic University of Korea

²Department of Ophthalmology, Seoul St. Mary's Hospital, College of Medicine, Catholic University of Korea

Correspondence: Jin A Choi, Department of Ophthalmology, St. Vincent's Hospital, College of Medicine, Catholic University of Korea, 93, Jungvu-daero Ji-dong, Paldal-gu, Suwon, Gyeonggi-do, 442-723, Korea; jinah616@catholic.ac.kr.

Submitted: March 9, 2016

Accepted: June 9, 2016

Citation: Jeon SJ, Kwon J-W, La TY, Park CK, Choi JA. Characteristics of retinal nerve fiber layer defect in nonglaucomatous eyes with type II diabetes. *Invest Ophthalmol Vis Sci*. 2016;57:4008–4015. DOI:10.1167/iov.16-19525

PURPOSE. To investigate the characteristics of retinal nerve fiber layer (RNFL) defects associated with type II diabetes.

METHODS. Forty nonglaucomatous eyes with type II diabetes and 54 eyes with early open angle glaucoma that exhibited a localized RNFL defect and 42 eyes from age- and sex-matched nondiabetic, nonglaucomatous controls were imaged with red-free fundus photography and optical coherence tomography (Cirrus HD-OCT, Carl Zeiss Meditec). The area under the receiver operating characteristic curves of eyes with diabetes was compared with that of eyes with glaucoma. When an RNFL defect on fundus photographs was identified in the quadrant, clock-hour, temporal-superior-nasal-inferior-temporal (TSNIT), deviation, and thickness maps, it was considered a true detection.

RESULTS. In eyes with diabetes, the RNFL defects were located more frequently in the superior hemisphere than they were in those with glaucoma ($P < 0.001$). The angular locations of RNFL defects in eyes with diabetes ($56.1 \pm 12.7^\circ$) were significantly farther from the fovea compared with those in glaucoma ($44.3 \pm 17.3^\circ$; $P < 0.001$); in addition, the width of RNFL defects in diabetes ($5.1 \pm 2.3^\circ$) was significantly narrower than those in glaucoma ($20.8 \pm 12.3^\circ$; $P < 0.001$). The best parameter discriminating RNFL defects in diabetes from those in glaucoma was width of RNFL defect (0.955), followed by rim area (0.844), and average RNFL (0.791). The thickness map showed a sensitivity (70%) and specificity (69.1%), superior to those of all other maps in eyes with diabetes.

CONCLUSIONS. The narrow width and identification of RNFL defect in thickness map obtained with Cirrus HD-OCT seems to be an effective tool for detecting RNFL defects in diabetes.

Keywords: diabetes mellitus, type 2, glaucoma, open-angle, tomography, optical coherence, nerve fibers, photography

The three major complications of diabetes are diabetic retinopathy (DR), nephropathy, and neuropathy. Among these, the primary focus has been on DR because it is the most sight-threatening complication of diabetes.^{1,2} However, renewed interest has focused on the neurodegenerative changes in the optic nerve in diabetes. Retinal nerve fiber layer (RNFL) abnormalities, manifesting as thinning or defects, are frequently encountered in subjects with diabetes.^{3–5} Thinning of the RNFL around the optic disc and macula thinning have been reported, and these changes often occur before the development of DR.^{3,6–9} Retinal nerve fiber layer defects, first described by Hoyt et al.¹⁰ 50 years ago, is one of the pathognomic findings in glaucomatous optic neuropathy. The RNFL defect may precede detectable changes on the optic disc and visual field (VF),¹¹ and RNFL-based assessments have been reported to be superior to optic disc-based assessments for the diagnosis of glaucoma.^{12,13}

Although both diseases accompany loss of RNFL, the underlying pathophysiologies of the two diseases are different. Structurally, RNFL loss in diabetes shows a relatively low correlation with the corresponding optic disc area compared to glaucoma, in which rim thinning in the optic disc corresponds to RNFL loss.¹⁴ In glaucoma, intraocular pressure is a major risk factor for the development of the disease¹⁵; however, in

diabetes, oxidative stress,⁶ accumulation of advanced glycation end products,¹⁶ and impaired retrograde axonal transport of retinal ganglion cells¹⁷ have been proposed to play a role, and the mechanism of RNFL defect in diabetes is not yet completely understood.

To date, there have been few reports regarding the structural differences of RNFL losses in the two diseases. Identifying the characteristics of RNFL defects in diabetes might provide objective criteria to discriminate from the RNFL defects in glaucoma and promote understanding of the underlying pathophysiology.

This present study aims to characterize RNFL defects associated with type II diabetes as an evidence of early neurodegeneration and to investigate the RNFL defects according to red-free fundus photograph and the relevant optical coherence tomography (OCT) findings in type II diabetes and glaucoma.

MATERIALS AND METHODS

Study Subjects

This was a cross-sectional study conducted according to the tenets of the Declaration of Helsinki and approved by the



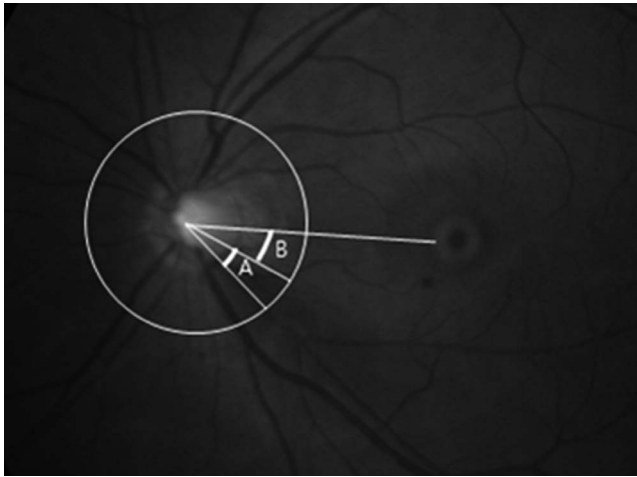


FIGURE 1. Measurement of angular location and width of a RNFL defect. First, a reference line connecting the center of the optic disc and the fovea was drawn to classify the RNFL distribution (superior or inferior) and to denote the starting line in angle measurement. The white circle is centered on the optic disc with a 3.46-mm diameter. The width of the RNFL defect was measured as the angle between the two lines from the center of the disc to the point that converged on the circle of 3.46 mm-diameter (angle A). The angular location of the RNFL defect was defined as the angle between the reference line and the borderline of the RNFL defect proximal to the reference line (angle B). The angular location was assessed starting with the line from the disc to the macula set at 0° and was divided into superior and inferior segments.

Institutional Review and Ethics Boards at St. Vincent's Hospital, Suwon, South Korea. Subjects with type II diabetes or early-stage primary open angle glaucoma (mean deviation [MD] > -6 dB) with an isolated superior or inferior hemifield RNFL defect on red-free fundus photograph and nondiabetic, non-glaucomatous controls who underwent ophthalmic examination between July 2014 and July 2015 at St. Vincent's Hospital, Catholic University of Korea, were included in this study.

All subjects underwent a complete ophthalmic examination, including measurement of visual acuity, Goldmann applanation tonometry, slit-lamp examination, gonioscopy, red-free RNFL photography (CF-60UD; Canon, Tokyo, Japan), standard automated perimetry using the 24-2 SITA program (Humphrey Visual Field Analyzer; Carl Zeiss Meditec, Inc., Dublin, CA, USA), and OCT (Cirrus OCT; Carl Zeiss Meditec, Inc.). All subjects were required to have a best-corrected visual acuity of 20/40 or better, a spherical equivalent within ± 5.0 diopters, and open angles on gonioscopy. Subjects with neurologic disease that could affect the VFs or a history of ocular surgery other than cataract extraction were excluded.

Subjects with diabetes were included if they had no signs of a glaucomatous optic disc (focal or generalized narrowing or disappearance of neuroretinal rim, disc hemorrhage, or cup-to-disc asymmetry > 0.2). They were required to have normal VF results during follow-up. A normal VF examination was defined as a glaucoma hemifield test result within normal limits and total and pattern standard deviation values associated with probabilities of normality greater than 5%. Based on the revised guidelines of the American Diabetes Association, diabetes was diagnosed in subjects with a fasting plasma glucose ≥ 126 mg/dL or symptoms of diabetes and random plasma glucose concentration ≥ 200 mg/dL.¹⁸ Diabetic retinopathy was graded by a retinal specialist (JWK). Severity of DR was categorized following the international clinical DR severity scales into five categories of nondiabetic retinopathy (NDR; equivalent to the Early Treatment Diabetic Retinopathy Study [ETDRS] scale

level 10), mild nonproliferative diabetic retinopathy (NPDR; equivalent to the ETDRS scale level 20), moderate NPDR (equivalent to the ETDRS scale level 35, 43, 47), severe NPDR (equivalent to the ETDRS scale level 53A-53E), and PDR (equivalent to the ETDRS scale level ≥ 61).¹⁹ Diabetes treatments were categorized as use of an oral agent, use of insulin, or lifestyle modifications alone. Subjects with PDR or neovascular glaucoma were excluded. Subjects with relevant feature of macula edema on spectral domain OCT were excluded. Subjects with associated interventions such as panretinal photocoagulation, intravitreal injection, or use of antiglaucoma eye drops were also excluded.

The control group included subjects with an intraocular pressure < 21 mm Hg, a normal optic disc appearance upon examination of color stereoscopic photographs (an intact neuroretinal rim without peripapillary hemorrhage, thinning, or localized pallor), the absence of any RNFL abnormality visible on red-free fundus photographs, normal VF test results, and no systemic disease such as diabetes or hypertension.

Subjects with glaucoma were included if they did not have a diagnosis of diabetes and had a glaucomatous disc appearance associated with a typical reproducible VF defect evident on SAP with MD more than -6 dB. A glaucomatous VF defect was defined as a glaucoma hemifield test result outside normal limits and the presence of at least three contiguous points in the pattern deviation plot with P values < 5%, with at least one point associated with a P value < 1% on two consecutive reliable VF examinations. When both eyes of a subject met the inclusion criteria, one eye was randomly selected.

Evaluation of RNFL Defects

The angular location and width of the RNFL defect were quantified using red-free RNFL photographs, as previously described.^{20,21} The photographs were obtained using a digital fundus camera at a 60° field of view. A reference line was drawn to connect the disc center and the fovea. The width of the RNFL defect was defined as the angle between two lines from the center of the disc to a point that converged on a circle of 3.46 mm diameter, which corresponds with the OCT scan circle. We defined the angular location of the RNFL defect as the angle between the reference line and the closer point of 3.46 mm diameter. The angular location was assessed starting with the line from the disc to the macula set at 0° and was divided into superior and inferior segments (Fig. 1). The image was analyzed using Image J (developed by Wayne Rasbands, National Institutes of Health, Bethesda, MD, USA) software.²² Retinal nerve fiber layer defects were independently evaluated in a blind manner by two clinicians (JAC and SJJ). Eyes with a disagreement in RNFL defect measurement between the two observers were excluded from this study. Eyes with multiple RNFL defects or diffuse RNFL defects were also excluded.

OCT Measurements

Imaging using an OCT was obtained after pupillary dilation to a minimum diameter of 5 mm and was acquired by a single, well-trained technician. Only accurate images with a signal strength ≥ 6 (10 = maximum) were included.

Cirrus OCT uses spectral-domain technology of an optic disc cube from 3D data that include a 6-mm² area centered on the optic disc. After generating an RNFL thickness map from the cube data set, the software automatically determines the center of the disc and then positions a 3.46-mm-diameter scan circle.^{23,24} Cirrus OCT provides the quadrant and clock-hour maps, temporal-superior-nasal-inferior-temporal (TSNIT) maps, and deviation maps based on the normative database and the thickness map, which is not based on the normative

TABLE 1. Baseline Characteristics and Parameters Obtained Using SD-OCT in Controls, Patients With Type 2 Diabetes, and Patients With Early-Stage-Open Angle Glaucoma

	Controls, <i>n</i> = 42	DM, <i>n</i> = 40	All Glaucoma, <i>n</i> = 54	<i>P</i> Value	Post Hoc Testing*
Demographics					
Age, y	51.8 ± 9.3	55.7 ± 12.0	54.3 ± 12.5	0.308†	
Female, <i>n</i> (%)	18 (42.3)	25 (62.5)	29 (53.7)	0.203‡	
Spherical equivalent, D	−0.87 ± 1.81	0.19 ± 1.76	−1.60 ± 2.66	0.116†	
Rim area, mm ²	1.3 ± 0.2	1.2 ± 0.2	0.9 ± 1.9	<0.001†	C > G, D > G
Disc area, mm ²	1.9 ± 0.3	2.1 ± 0.4	2.1 ± 0.5	0.079†	D > C
Average RNFL thickness, μm	98.31 ± 7.93	91.57 ± 10.89	80.31 ± 8.16	<0.001†	C > D > G
Quadrant map, μm					
Superior	126.45 ± 19.07	113.28 ± 18.12	99.01 ± 15.27	<0.001†	C > D > G
Inferior	129.33 ± 11.71	113.18 ± 18.54	93.68 ± 18.05	<0.001†	C > D > G
Temporal	71.30 ± 8.48	68.55 ± 10.87	64.22 ± 10.04	0.002†	C > G
Nasal	67.19 ± 7.27	69.68 ± 13.33	64.64 ± 9.94	0.070†	

C, control; D, type II diabetes; G, all glaucoma.

* Bonferroni post hoc test.

† 1-way ANOVA.

‡ χ^2 test.

data. Cirrus software automatically provides a classification—within normal limits, borderline, or outside normal limits—derived by comparison of RNFL thickness data with the internal database of a healthy, age-matched normal population, with a corresponding color coding scheme. A result is considered abnormal when the RNFL thickness value falls below a nominated percentile of the intrinsic normative database information as follows: outside the 99% confidence interval (CI; coded as a red band) or between the 95% and 99% CIs of the normative database (coded as a yellow band).

Using the five maps provided by Cirrus OCT (quadrant, clock-hour, TSNIT, deviation, and thickness maps), we defined the “abnormal” finding in each OCT map as “detection of a photographic RNFL defect” when it corresponded to the location of the RNFL defect in the red-free fundus photograph. The definitions of “abnormal finding” in each map are as follows: (1) The red or yellow sector in the quadrant and clock-hour maps, (2) the points on the TSNIT graph located within the red band (outside the 95% normal limit) or with the red (outside the 99% normal limit),²⁵ (3) the presence of a yellow or red area with a size > 10 pixels in the deviation map,^{26,27} and (4) the presence of a blue area in the thickness map.²⁶ The evaluation of RNFL defects on fundus photography and each OCT map were independently evaluated in a random order and blinded fashion. Besides the RNFL thickness measurements, two optic nerve head (ONH) parameters (disc area and rim area) were also measured.

Statistical Analysis

Statistical analyses were performed with SPSS version 18.0 (SPSS, Inc., Chicago, IL, USA) and MedCalc software (Mariakerke, Belgium). *P* < 0.05 was considered significant. 1-way ANOVA with Bonferroni post hoc tests and χ^2 tests were used to compare the clinical characteristics among nondiabetic, nonglaucomatous controls and diabetes mellitus (DM) and glaucoma groups. The distribution of RNFL defects in DM and glaucoma subjects were compared using the χ^2 test, and the angular location and width of RNFL defects were compared using Student's *t*-tests.

The Mantel-Haenszel χ^2 test was used to evaluate if the detection capabilities of each OCT map were affected by the disease (DM and glaucoma), and the McNemar test was used to compare the detection rate of the OCT maps. The area under

the receiver operating characteristic (AUROC) curves was calculated to evaluate the diagnostic ability of parameters of red-free fundus photograph and spectral-domain-OCT (SD-OCT) device in the DM and glaucoma groups and to evaluate the discriminating ability of RNFL defects in DM from those in glaucoma. The differences of AUROC were tested using the method of Hanley and McNeil.²⁸ To evaluate the diagnostic capabilities of each OCT map in detecting photographic RNFL defects, the sensitivity and specificity percentage were calculated in each OCT map. Subgroup analyses were performed in patients with very early stage glaucoma with MD more than −3 dB.

RESULTS

A total of 333 patients with diabetes received an ophthalmic examination between July 2014 and July 2015. Among them, 199 patients having glaucomatous optic disc or glaucomatous VF loss were excluded. Among them, 60 were excluded due to no evidence of RNFL defect, and 28 subjects were excluded because of multiple or ambiguous RNFL defect. Six eyes with a disagreement in RNFL defect measurement between the two observers were excluded from this study. Finally, 40 eyes of 40 subjects with type II diabetes and 54 eyes of 54 subjects with glaucoma with an isolated superior or inferior hemifield RNFL defect on red-free fundus photograph, and 42 eyes of 42 nondiabetic, nonglaucomatous controls were enrolled. There were no statistically significant differences in age, sex, or spherical equivalent among the groups (*P* = 0.308, 0.203, and 0.116, respectively, Table 1). The diabetes mellitus group had 13 (32.5%) subjects with no DR, 12 (30%) subjects with mild NPDR, 8 (20%) subjects with moderate NPDR, and 7 (17.5%) subjects with severe NPDR. No subjects in the DM group had PDR. The average duration of diabetes was 12.5 ± 7.3 years. The mean fasting blood glucose, HbA1c, and eGFR were 148.9 ± 61.9 mg/mL, 8.2 ± 1.8 g/dL, and 99.9 ± 24.9 mL/min/1.73 m², respectively. In the DM group, 20 (50%) subjects were treated with oral agents, 9 (22.5%) with insulin, and 1 (5.0%) with life style modification alone.

The average, superior, inferior, and temporal quadrant RNFL thickness and rim area measured by OCT was significantly different among the groups (*P* < 0.001). Post hoc testing revealed that the average, superior, and inferior quadrant RNFL were thinnest in subjects with glaucoma, followed by those

TABLE 2. Distribution of RNFL Defects in Patients With DM and Patients With Glaucoma Evaluated by Red-Free Fundus Photographs

Characteristics	DM, <i>n</i> = 40	Glaucoma, <i>n</i> = 54	<i>P</i> Value
Location, superior:inferior	34:6	22:32	<0.001*
Angle, degrees	56.1 ± 12.7	44.3 ± 17.3	<0.001†
Width, degrees	5.1 ± 2.3	20.8 ± 12.3	<0.001†

* χ^2 test.† Student's *t*-test.

with diabetes, and controls. The rim area was significantly thinner in subjects with glaucoma, compared with control and diabetes (Table 1).

Table 2 shows the comparison of the characteristics of RNFL defects on red-free fundus photographs. Retinal nerve fiber layer defects of the DM group were more commonly found in the superior hemisphere than the inferior hemisphere ($P < 0.001$). The angular location of the RNFL defects in the DM group ($56.1 \pm 12.7^\circ$) was significantly farther from the fovea, compared with those in the glaucoma group ($44.3 \pm 17.3^\circ$; $P < 0.001$). The average width of RNFL defects in the DM group ($5.1 \pm 2.3^\circ$) was significantly narrower than those in the glaucoma group ($20.8 \pm 12.3^\circ$; $P < 0.001$).

All OCT maps showed better detection ability in the glaucoma group compared with the DM group (all P value < 0.05; Fig. 2A). In very early glaucoma subgroup (MD > -3 dB), the quadrant, clock-hour, TSNIT, and deviation maps showed better detection ability in the all glaucoma group compared with the DM group (all P value < 0.05), whereas the differences were not significant for the thickness map ($P = 0.074$; Fig. 2B).

The area under the receiver operating characteristic values of the DM and glaucoma groups were calculated in comparison with controls (Table 3). The area under the receiver operating characteristic values of average RNFL thickness, superior, inferior, nasal quadrant RNFL thickness and rim area were significantly lower in the DM group than in the glaucoma group (all $P < 0.05$). In the DM group, inferior quadrant thickness had the largest AUROC value, which was followed by superior quadrant thickness. No statistical differences were noted between the AUROC of the inferior and superior quadrant RNFL thickness ($P = 0.329$).

Figure 3 shows the receiver operating characteristic curves of best parameters of red-free fundus photograph and SD-OCT device, discriminating RNFL defects in type II diabetes from

those in glaucoma. The best parameter discriminating RNFL defects in type II diabetes from those in open angle glaucoma was width of RNFL defect (0.955), followed by rim area (0.844) and average RNFL (0.791; Fig. 3A). There were statistically significant differences between the AUROC of the width of RNFL defect and that of the rim area ($P = 0.006$). No statistical differences were noted between the AUROC of the rim area and that of the average RNFL thickness ($P = 0.208$). In very early glaucoma subgroup (MD > -3 dB), the best parameters for discriminating type II diabetes from open angle glaucoma was also the width of RNFL defect (0.955), followed by the rim area (0.892) and the average RNFL (0.799; Fig. 3B).

Sensitivity and specificity for detecting RNFL defects using each OCT map are shown in Table 4. In the DM group, the overall sensitivities were much lower than those in the glaucoma group. In the DM group, the sensitivity was lowest in the quadrant map and highest in the thickness map. The thickness map showed highest sensitivity in the glaucoma group and also in the very early glaucoma subgroup.

DISCUSSION

There has been renewed interest in neurodegenerative changes in early diabetes. Optical coherence tomography of the retina and around the ONH can quantify neurodegenerative changes in subjects with diabetes.¹⁴ Many studies have demonstrated that, even in the absence of vascular changes, several layers in the retina and RNFL thickness around the optic disc become significantly thinner in eyes with type II diabetes compared with those without diabetes.^{8,9} Our study demonstrated that average RNFL thickness and sector RNFL thickness in superior and inferior quadrants in diabetes were significantly thinner than those of nondiabetic, nonglaucomatous controls (Table 1).

Several studies regarding preferential RNFL losses in diabetes showed that the most frequent location was the superior hemisphere,⁶⁻⁸ whereas others reported that both superior and inferior RNFL thickness were decreased with progression of DR.²⁹⁻³¹ In this study, 34 (85%) diabetic subjects had photographic RNFL defects on the superior hemisphere (Table 2). On the contrary, the highest AUROC value was found in the inferior quadrant followed by superior quadrant RNFL (Table 3). It may be associated with the relative differences of crowding of axonal density between superior and inferior hemisphere.³² Hood et al.³² reported that the relative inferior location of fovea to ONH results in the crowding of the retinal ganglion cell axons in the inferior temporal side of the ONH. Thus, inferior RNFL is normally thicker than superior RNFL and the distribution of RNFL in superior hemisphere is relatively

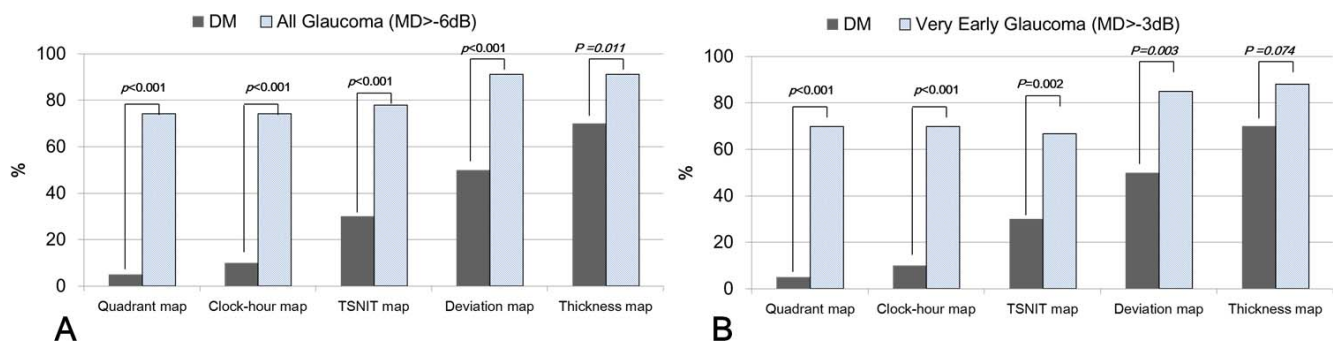


FIGURE 2. Detection of photographic RNFL defects by each map of Cirrus OCT in patients with type II diabetes and patients with open angle glaucoma. (A) All OCT maps showed better detection ability in the glaucoma group compared with the DM group (all $P < 0.05$). (B) In very early glaucoma subgroup (MD > -3 dB), the quadrant, clock-hour, TSNIT, and deviation maps showed better detection ability in the all glaucoma group compared with the DM group (all $P < 0.05$), whereas the differences were not significant for the thickness map ($P = 0.074$).

TABLE 3. AUROC Curve Values of OCT Parameters Among Healthy Controls and Patients With DM and Among Healthy Controls and Patients With Glaucoma

	AUROC Curve (95% CI)		
	DM	Glaucoma	P Value
Average RNFL thickness	0.678 (0.563–0.793)	0.938 (0.870–0.977)	<0.001
Superior RNFL thickness	0.684 (0.569–0.798)	0.888 (0.808–0.944)	0.001
Inferior RNFL thickness	0.761 (0.658–0.865)	0.947 (0.882–0.982)	0.001
Temporal RNFL thickness	0.571 (0.445–0.697)	0.690 (0.587–0.780)	0.151
Nasal RNFL thickness	0.425 (0.296–0.554)	0.594 (0.489–0.693)	0.048
Rim area	0.623 (0.509–0.728)	0.922 (0.849–0.967)	<0.001

wider compared with that in inferior hemisphere.³⁵ Therefore, the ability of inferior RNFL thickness discriminating normal from abnormal condition seems to be better than that of superior RNFL thickness.

It is interesting that in subjects with type II diabetes and photographic RNFL defect, 52.5% of subjects revealed no DR or mild NPDR, although the average duration of the disease was relatively long (12.5 ± 7.3 years). There is increasing recognition that diabetes is associated with early neurodegeneration and the impairment in neurovascular coupling mechanism occurs as an early event in the pathogenesis of DR. The response of retinal vessel dilatation to visual stimulation, one of the methods for the assessment of neurovascular coupling in the ONH and retina, was impaired in subjects with clinically detectable DR, and it was progressively decreased with more severe stage of DR.³⁴ Even in diabetes without clinically visible retinopathy, neural and neurovascular dysfunction were detected.³⁵ Lasta et al.³⁶ reported that neurovascular coupling was reduced in type I diabetes before the alteration of neural activity. Injuries in neurovascular coupling mechanism, which is important in the brain homeostasis, are also present in pathologic conditions such as stroke, subarachnoid hemorrhage, and dementias.³⁷ Recent surveys have found that localized RNFL defects are also associated with neurodegenerative diseases such as stroke³⁸ or small vessel disease³⁹; they are also associated with arterial hypertension.⁴⁰ In this regard, RNFL defect in diabetes seems to be one manifestation other than DR, which could be used as one of the surrogate markers

of impaired neurovascular coupling in neurodegenerative disease.

Intriguingly, we found that RNFL defects detected by red-free photographs in DM subjects were narrower than those of glaucoma subjects as shown in representative cases (Table 2; Fig. 4). The width of RNFL defect was the best parameter discriminating RNFL defects in type II diabetes from those in open angle glaucoma and very early stage glaucoma subgroup (Figs. 3A, 3B). It suggests that width of RNFL defects (Youden's index; 6.6°) can be useful in identifying diabetes-associated RNFL defects in clinical practice.

Suh et al.¹⁴ showed that nonprogressive RNFL defects in diabetic subjects could be well differentiated from those in glaucoma by preservation of neuroretinal rim. Lim et al.²⁹ also reported that the ONH cupping did not increase with severity of disease classification in diabetes. In agreement with their studies, rim area measured with OCT was the second-best parameters discriminating RNFL defects in diabetes from those in open angle glaucoma (Fig. 3). Optic neuropathy has different pathophysiology when it is caused by diabetes versus glaucoma. In glaucoma, the ganglion cells in the lamina cribrosa are damaged in the process of compression with large pores,^{41,42} which results in characteristic cupping of the ONH. In this regard, the size and depth of ONH and RNFL damage in glaucoma can be more severe than diabetic RNFL loss.

The possibility of identification of RNFL defects by all OCT maps were significantly lower in the diabetes group (all $P < 0.05$; Fig. 2A). However, the detection rate of RNFL defects on

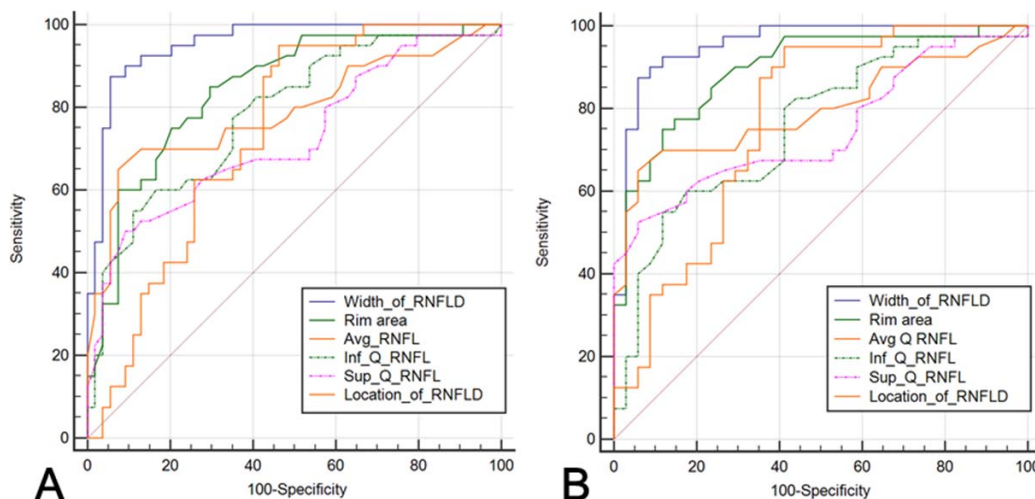


FIGURE 3. Receiver operating characteristic (ROC) curves of best parameters of red-free fundus photograph and SD-OCT device, discriminating RNFL defects in type II diabetes from those in glaucoma. The best parameters were width of RNFL defect (0.955), followed by rim area (0.844), and average RNFL thickness (0.791). There were statistically significant differences between AUROC of the width of RNFL defect and that of the rim area ($P = 0.006$). **(B)** In very early glaucoma subgroup (MD > -3 dB), the best parameter discriminating type II diabetes from glaucoma were width of RNFL defect (0.955), followed by rim area (0.892) and average RNFL (0.799).

TABLE 4. Overall Sensitivity and Specificity of Each Map of Cirrus OCT for Detecting Localized RNFL Defects

	DM, n = 40		All Glaucoma (> -6 dB), n = 54		Very Early Glaucoma (> -3 dB), n = 33	
	Sensitivity, %	Specificity, %	Sensitivity, %	Specificity, %	Sensitivity, %	Specificity, %
Quadrant map	5.0 (1.4-16.5)	95.2 (84.2-98.7)	74.1 (61.1-83.4)	95.2 (84.2-98.7)	69.7 (52.7-82.6)	95.2 (84.2-98.7)
Clock-hour map	10.0 (4.0-23.1)	83.3 (69.4-91.7)	74.1 (61.1-83.4)	83.3 (69.0-91.7)	69.7 (52.7-82.6)	83.3 (69.4-91.7)
TSNIT map	30.0 (18.1-45.4)	97.6 (87.7-99.6)	77.8 (65.1-86.8)	97.6 (87.7-99.6)	66.7 (49.6-80.3)	97.6 (87.7-99.6)
Deviation map	50.0 (35.2-64.8)	71.4 (56.4-82.8)	90.7 (80.1-96.0)	71.4 (56.4-82.8)	84.9 (69.1-93.4)	71.4 (56.4-82.8)
Thickness map	70.0 (54.6-81.9)	69.1 (53.4-81.0)	90.7 (80.1-96.0)	69.1 (54.0-81.0)	87.9 (72.7-95.2)	69.1 (54.0-81.0)

the thickness map was not significantly different between subjects with diabetes and those with glaucoma in very early glaucoma subgroup ($P = 0.074$; Fig. 2B). This seems to be related with the fact that the thickness map is not based on normative data, whereas other OCT maps are based on the internal normative database. This indicates that the depth of RNFL defects in diabetes is relatively shallow, and they can be detected using red-free fundus photographs and the OCT thickness map, which detects RNFL defects based on relative difference in thickness from adjacent structures. However, RNFL defects in diabetes are not deep enough to be assessed as outside the normal range in OCT. The thickness map showed a sensitivity (70%) and specificity (69.1%) superior to those of all other maps in eyes with diabetes (Table 4). The significantly lower values for the area under receiver operating curves in subjects with diabetes compared with glaucoma subjects also support this finding (Table 3).

The strength of this study is that we characterized RNFL defects in diabetes by comparison with those in age-matched nondiabetic, nonglaucomatous controls and primary open

angle glaucoma. However, potential limitations of our study should be mentioned. First, this study was clinically based and did not use population-based screening. The participants were all Korean, and participants with PDR or neovascular glaucoma were excluded. Secondly, to avoid possible overlap between DM and glaucoma groups, we included type II diabetic subjects with nonglaucomatous optic discs showing a normal VF. In addition, subjects with diabetes were excluded from the glaucoma group. However, since diabetes is a probable risk factor of glaucoma, there is a possibility that nonglaucomatous eyes with diabetes may develop glaucomatous changes of the optic disc. A normal RNFL thickness profile is affected by various factors such as age, ethnicity, axial length, and optic disc area, resulting in considerable variation in RNFL thickness in the normal population. Conditions such as lens opacities and dry eye could affect RNFL thickness profile. In this study, we utilized Cirrus OCT scans with signal strength greater or equal to 6. However, there are still possibilities that low signal strength associated with in mild cataracts could affect the RNFL thickness. Also, using the entire region of the deviation

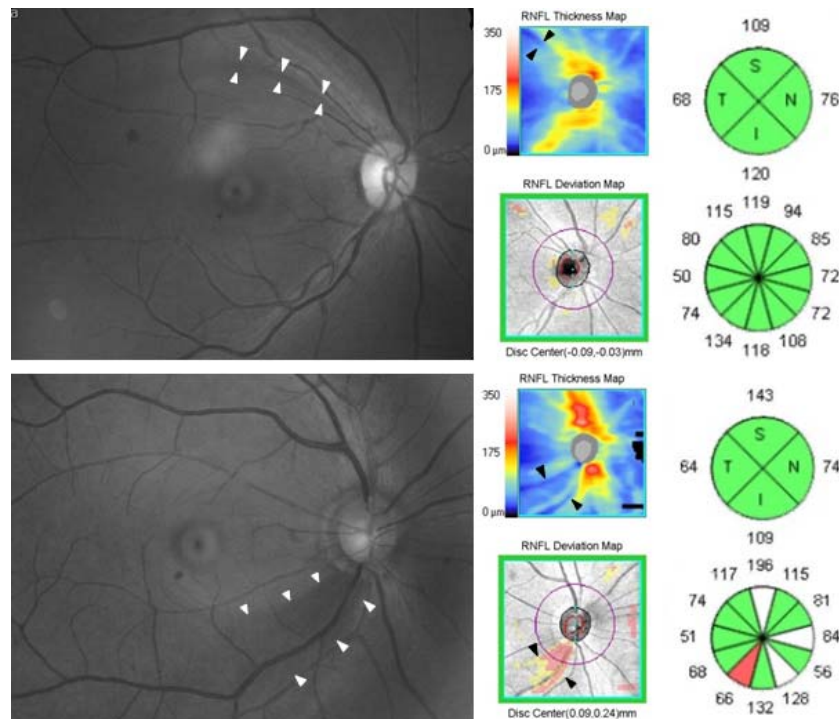


FIGURE 4. Representative cases showing the characteristics of RNFL defects in type II diabetes and open angle glaucoma patients. (Upper) A 36-year-old female with type II diabetes. In red-free fundus photography, the RNFL defect seen on the superior hemisphere is narrow (5°) and located far from the fovea with an angular location of 52°. The superotemporal RNFL defect is only detected in the thickness map (black arrow). (Lower) A 61-year-old male with normal tension glaucoma. The RNFL defect on the inferior hemisphere is wide (39°) and located closer to the fovea with an angular location of 43°. The thickness map, the deviation map, and the clock-hour map detected the inferotemporal RNFL defect. The white arrows demarcate the border of the RNFL defect.

map and the thickness map as parameters may be influenced by artifacts such as vitreous opacities, magnification errors due to high myopia. Further prospective studies are warranted to investigate changes in nonglaucomatous RNFL defects in diabetes over time. Finally, subjects with type II diabetes and RNFL defects were included in the study. Thus, many diabetic patients were excluded, which may cause a possible statistical bias.

In conclusion, subjects with type II diabetes and photographic RNFL defect, 52.5% of subjects revealed no DR or mild NPDR. The RNFL defects of DM subjects were differentiated from early glaucomatous RNFL defects. The RNFL defects in diabetes were located predominantly in the superior hemisphere and tended to be narrower, shallower, and farther from the fovea compared to those in glaucoma. The thickness map in Cirrus OCT seems to be an effective tool for detecting RNFL defects in diabetes.

Acknowledgments

The authors acknowledge the financial support of the Catholic Medical Center Research Foundation, made in program year 2014, and the St. Vincent's Hospital, Research Institute of Medical Science Foundation (SVHR-2015-09). The authors alone are responsible for the content and writing of the paper.

Disclosure: **S.J. Jeon**, None; **J.-W. Kwon**, None; **T.Y. La**, None; **C.K. Park**, None; **J.A. Choi**, None

References

- De Clerck EEB, Schouten JSAG, Berendschot TTJM, et al. New ophthalmologic imaging techniques for detection and monitoring of neurodegenerative changes in diabetes: a systematic review. *Lancet Diabetes Endocrinol*. 2015;3:653-663.
- Chhablani J, Sharma A, Goud A, et al. Neurodegeneration in type 2 diabetes: evidence from spectral-domain optical coherence tomography. *Invest Ophthalmol Vis Sci*. 2015;56:6333-6338.
- Chihara E, Matsuoka T, Ogura Y, Matsumura M. Retinal nerve fiber layer defect as an early manifestation of diabetic retinopathy. *Ophthalmology*. 1993;100:1147-1151.
- Choi JA, Ko SH, Park YR, Jee DH, Ko SH, Park CK. Retinal nerve fiber layer loss is associated with urinary albumin excretion in patients with type 2 diabetes. *Ophthalmology*. 2015;122:976-981.
- Jie R, Xu L, Wang Y, et al. Ten-year incidence of retinal nerve fiber layer defects: the Beijing Eye Study 2001/2011. *Invest Ophthalmol Vis Sci*. 2015;56:5118-5124.
- Lopes de Faria JM, Russ H, Costa VP. Retinal nerve fibre layer loss in patients with type 1 diabetes mellitus without retinopathy. *Br J Ophthalmol*. 2002;86:725-728.
- Ozdek S, Lonnaville YH, Onol M, Yetkin I, Hasanreisoglu BB. Assessment of nerve fiber layer in diabetic patients with scanning laser polarimetry. *Eye (Lond)*. 2002;16:761-765.
- Sugimoto M, Sasoh M, Ido M, Wakitani Y, Takahashi C, Uji Y. Detection of early diabetic change with optical coherence tomography in type 2 diabetes mellitus patients without retinopathy. *Ophthalmologica*. 2005;219:379-385.
- Zhao L, Wang YX, Zhang W, et al. Localized retinal nerve fiber layer defects detected by optical coherence tomography: the Beijing eye study. *PLoS One*. 2013;8:e68998.
- Hoyt WF, Schlicke B, Eckelhoff RJ. Fundoscopic appearance of a nerve-fibre-bundle defect. *Br J Ophthalmol*. 1972;56:577-583.
- Tuulonen A, Lehtola J, Airaksinen PJ. Nerve fiber layer defects with normal visual fields. Do normal optic disc and normal visual field indicate absence of glaucomatous abnormality? *Ophthalmology*. 1993;100:587-597, discussion 597.
- Leung C, Medeiros F, Zangwill L, et al. American Chinese glaucoma imaging study: a comparison of the optic disc and retinal nerve fiber layer in detecting glaucomatous damage. *Invest Ophthalmol Vis Sci*. 2007;48:2644-2652.
- Medeiros F, Vizzeri G, Zangwill L, Alencar L, Sample P, Weinreb R. Comparison of retinal nerve fiber layer and optic disc imaging for diagnosing glaucoma in patients suspected of having the disease. *Ophthalmology*. 2008;115:1340-1346.
- Suh MH, Kim SH, Park KH, Yu HG, Huh JW, Kim DM. Optic disc rim area to retinal nerve fiber layer thickness correlation: comparison of diabetic and normal tension glaucoma eyes. *Jpn J Ophthalmol*. 2013;57:156-165.
- Quigley H. Glaucoma. *The Lancet*. 2011;377:1367-1377.
- Amano S, Kaji Y, Oshika T, et al. Advanced glycation end products in human optic nerve head. *Br J Ophthalmol*. 2001;85:52-55.
- Zhang L, Ino-ue M, Dong K, Yamamoto M. Retrograde axonal transport impairment of large- and medium-sized retinal ganglion cells in diabetic rat. *Curr Eye Res*. 2000;20:131-136.
- Diagnosis and classification of diabetes mellitus. *Diabetes Care*. 2004;27(suppl 1):S5-S10.
- Wilkinson CP, Ferris F, Klein R, et al. Proposed international clinical diabetic retinopathy and diabetic macular edema disease severity scales. *Ophthalmology*. 2003;110:1677-1682.
- Woo SJ, Park KH, Kim DM. Comparison of localised nerve fibre layer defects in normal tension glaucoma and primary open angle glaucoma. *Br J Ophthalmol*. 2003;87:695-698.
- Yamashita T, Nitta K, Sonoda S, Sugiyama K, Sakamoto T. Relationship between location of retinal nerve fiber layer defect and curvature of retinal artery trajectory in eyes with normal tension glaucoma. *Invest Ophthalmol Vis Sci*. 2015;56:6190-6195.
- Schneider CA, Rasband WS, Eliceiri KW. NIH Image to ImageJ: 25 years of image analysis. *Nat Methods*. 2012;9:671-675.
- Sung KR, Kim DY, Park SB, Kook MS. Comparison of retinal nerve fiber layer thickness measured by Cirrus HD and Stratus optical coherence tomography. *Ophthalmology*. 2009;116:1264-1270.
- Kim NR, Lim H, Kim JH, Rho SS, Seong GJ, Kim CY. Factors associated with false positives in retinal nerve fiber layer color codes from spectral-domain optical coherence tomography. *Ophthalmology*. 2011;118:1774-1781.
- Kim KE, Kim SH, Jeoung JW, Park KH, Kim TW, Kim DM. Comparison of ability of time-domain and spectral-domain optical coherence tomography to detect diffuse retinal nerve fiber layer atrophy. *Jpn J Ophthalmol*. 2013;57:529-539.
- Hwang Y, Kim Y, Kim H, Sohn Y. Ability of cirrus high-definition spectral-domain optical coherence tomography clock-hour, deviation, and thickness maps in detecting photographic retinal nerve fiber layer abnormalities. *Ophthalmology*. 2013;120:1380-1387.
- Kim N, Lim H, Kim J, Rho S, Seong G, Kim C. Factors associated with false positives in retinal nerve fiber layer color codes from spectral-domain optical coherence tomography. *Ophthalmology*. 2011;118:1774-1781.
- Hanley JA, McNeil BJ. The meaning and use of the area under a receiver operating characteristic (ROC) curve. *Radiology*. 1982;143:29-36.
- Lim MC, Tanimoto SA, Furlani BA, et al. Effect of diabetic retinopathy and panretinal photocoagulation on retinal nerve fiber layer and optic nerve appearance. *Arch Ophthalmol*. 2009;127:857-862.
- Takahashi H, Goto T, Shoji T, Tanito M, Park M, Chihara E. Diabetes-associated retinal nerve fiber damage evaluated with scanning laser polarimetry. *Am J Ophthalmol*. 2006;142:88-94.

31. Park H, Kim I, Park C. Early diabetic changes in the nerve fibre layer at the macula detected by spectral domain optical coherence tomography. *Br J Ophthalmol*. 2011;95:1223-1228.
32. Hood DC, Raza AS, de Moraes CG, Liebmann JM, Ritch R. Glaucomatous damage of the macula. *Prog Retin Eye Res*. 2013;32:1-21.
33. Choi JA, Park HY, Jung KI, Hong KH, Park CK. Difference in the properties of retinal nerve fiber layer defect between superior and inferior visual field loss in glaucoma. *Invest Ophthalmol Vis Sci*. 2013;54:6982-6990.
34. Lim LS, Ling LH, Ong PG, et al. Dynamic responses in retinal vessel caliber with flicker light stimulation in eyes with diabetic retinopathy. *Invest Ophthalmol Vis Sci*. 2014;55:5207-5213.
35. Leclaire-Collet A, Audo I, Aout M, et al. Evaluation of retinal function and flicker light-induced retinal vascular response in normotensive patients with diabetes without retinopathy. *Invest Ophthalmol Vis Sci*. 2011;52:2861-2867.
36. Lasta M, Pemp B, Schmidl D, et al. Neurovascular dysfunction precedes neural dysfunction in the retina of patients with type 1 diabetes. *Invest Ophthalmol Vis Sci*. 2013;54:842-847.
37. Muoio V, Persson PB, Sendeski MM. The neurovascular unit: concept review. *Acta Physiol (Oxf)*. 2014;210:790-798.
38. Wang D, Li Y, Wang C, et al. Localized retinal nerve fiber layer defects and stroke. *Stroke*. 2014;45:1651-1656.
39. Kim M, Park K, Kwon J, Jeoung J, Kim T-W, Kim D. Retinal nerve fiber layer defect and cerebral small vessel disease. *Invest Ophthalmol Vis Sci*. 2011;52:6882-6886.
40. Xu L, Zhou J, Wang S, et al. Localized retinal nerve fiber layer defects and arterial hypertension. *Am J Hypertension*. 2013;26:511-517.
41. Jonas JB, Mardin CY, Schlotzer-Schrehardt U, Naumann GO. Morphometry of the human lamina cribrosa surface. *Invest Ophthalmol Vis Sci*. 1991;32:401-405.
42. Morrison JC, Cepurna Ying Guo WO, Johnson EC. Pathophysiology of human glaucomatous optic nerve damage: insights from rodent models of glaucoma. *Exp Eye Res*. 2011;93:156-164.